Optoelectronic sensor for the measurement of dissolved oxygen in aquaculture

Hailen Andrea Chacón López

Natalia Estefanía Cruz Castillo

Jose Luis Parra Villamizar

Undergraduate thesis presented as a requirement to obtain the degree of

Electronic Engineer

Director:

Rodolfo Villamizar Mejía

Dr.

Co-director:

Omar Javier Tijaro Rojas

Dr.

Universidad Industrial de Santander

Faculty of Physical-Mechanical Engineering

School of Electrical, Electronic and Telecommunications Engineering

Bucaramanga

2026

Acknowledgments

First and foremost, I thank God for the opportunity to walk this path and reach this point. I am deeply grateful to my parents, Heli and Elsa, for their unconditional love and support throughout this journey. Thank you for every sacrifice, every piece of advice, and for always being there every step of the way. To my sister, Erika, thank you for being the support I so often needed, for understanding me, helping me, advising me, and offering a shoulder to lean on during the most difficult moments. To my aunts, Dora and Leydi, thank you for accompanying me throughout these years and for always welcoming me into your home. To my cousin Sebastián, thank you for being my playmate and for inspiring me to become a better person.

I would also like to thank my cats, Pelusa, Zeus, Aron, and Hades, for keeping me company during countless nights of study and making the days of hard work and exhaustion more bearable. To my friends, thank you for making my university experience more enjoyable, for the hours of studying together, the shared experiences, and all the memories we created along the way. To those who shared this undergraduate thesis project with me, thank you for welcoming me into your project; it is immensely rewarding to know that we were able to deliver a piece of work that we can all be proud of. Finally, to my girlfriend, thank you for being the driving force my life needed, for encouraging me to keep moving forward, and for believing in me.

With appreciation, **Hailen Andrea Chacón López**

Acknowledgments

First, I would like to thank God for everything He has given me and, especially, for the people I think of while writing these lines.

I would like to thank my family, who taught me the importance of education from an early age and supported me throughout this entire university journey. Thank you for always looking after my well-being, for visiting me when I could not travel, for understanding my absences, and for being present even in the most difficult moments.

I would also like to thank my cats, who accompanied me throughout these years. They were there during my days of virtual classes and later waited for my return home after long days at the university. Although they probably did not know it, they made many difficult days more bearable simply with their presence.

I also thank God for having placed in my path a person who was an immense support during this stage, someone who encouraged me in moments of exhaustion, motivated me to be a better person every day, and was there when I most needed companionship and support.

I would also like to thank the friends I made before and during university: those who have been with me since school, those I met in Barrancabermeja and shared the experience of arriving in Bucaramanga, and those I met in this city. Thank you for the study sessions, conversations, trips, and countless moments that made this journey more meaningful and enjoyable. Likewise, I would like to thank the rugby team for being a space for learning, companionship, and experiences that enriched my university life.

Finally, I would like to thank my thesis teammates, with whom it was possible to bring this project to a successful conclusion. This achievement would not have been possible without the shared effort, commitment, and dedication throughout the entire process.

With appreciation, **Natalia Estefania Cruz Castillo**

Acknowledgments

First and foremost, I would like to express my deepest gratitude to my family for their unconditional love, support, and encouragement throughout my university journey.

To my parents, thank you for always being there for me, for your guidance, patience, and constant support during both the challenges and achievements of these years. To my godmother, thank you for your care and unwavering presence; your support has meant more to me than words can express. To my sister, thank you for your kindness and unconditional encouragement throughout this process.

I would also like to thank Manchas, my beloved cat, for her companionship during countless hours of studying and writing. Her presence brought comfort and joy during difficult moments.

I thank God for giving me the strength, opportunities, and perseverance to achieve my goals and for placing extraordinary people in my life along the way.

To my partner, thank you for your love, patience, and support throughout this journey. Your encouragement helped me grow both personally and professionally.

To my friends and classmates, thank you for the experiences, lessons, and friendships that shaped my university years. You helped me grow academically, personally, and socially in ways I will always value.

Finally, I would like to thank my professors for their guidance, knowledge, and confidence in my abilities. Their support played an important role in my development as an engineer and as a person.

To everyone who accompanied me on this journey, thank you. This achievement would not have been possible without your support.

With appreciation, **Jose Luis Parra Villamizar**

Table of Contents

Pág.

List of Figures

Pág.

List of Tables

Pág.

List of Appendices

Pág.

Resumen

Título: Sensor optoelectrónico para la medición de oxígeno disuelto en acuicultura [*]

Autores: Hailen Andrea Chacón López,

Natalia Estefanía Cruz Castillo,

Jose Luis Parra Villamizar[**]

Palabras clave: Oxígeno disuelto, sensor optoelectrónico, espectroscopía de absorción, acuicultura, Internet de las Cosas (IoT), regresión lineal múltiple (MLR), monitoreo de calidad del agua.

Descripción:

Los sistemas acuícolas requieren monitoreo continuo del oxígeno disuelto para garantizar la supervivencia y productividad de las especies cultivadas; sin embargo, los sensores comerciales disponibles presentan altos costos y limitada accesibilidad para pequeños productores. Este trabajo presenta el diseño e implementación de un sensor optoelectrónico de bajo costo para la estimación de oxígeno disuelto en agua. El sistema utiliza una fuente de luz, un sensor multiespectral y variables complementarias como temperatura y presión, a partir de las cuales se adquieren señales ópticas en condiciones experimentales reales. Estas señales son procesadas mediante la ecuación de absorbancia para relacionar la intensidad óptica medida con las propiedades del medio acuoso. Las variables resultantes se emplean como entradas de un modelo de aprendizaje supervisado que relaciona las mediciones con valores de referencia obtenidos mediante un instrumento patrón. El desempeño del sistema fue evaluado utilizando una partición de los datos experimentales en conjuntos de entrenamiento (70%) y prueba (30%), obtenidos bajo condiciones reales de medición, logrando un coeficiente de determinación de $R^2 = 0.9582$ y un error cuadrático medio de $RMSE = 0.3801$ mg/L durante la evaluación offline. Además, el sistema integra una plataforma de visualización en tiempo real basada en Grafana, permitiendo el monitoreo continuo de las variables medidas. El sistema propuesto representa una alternativa accesible y escalable para el monitoreo de la calidad del agua, con potencial para contribuir a la optimización de los procesos productivos en sistemas acuícolas de pequeña y mediana escala.

---

[*] Tesis de pregrado

[**] Facultad de Ingenierías Físico-Mecánicas. Escuela de Ingenierías Eléctrica, Electrónica y de Telecomunicaciones. Director: Rodolfo Villamizar Mejía. Doctor. Codirector: Omar Javier Tijaro Rojas. Doctor.

Abstract

Title: Optoelectronic Sensor for Dissolved Oxygen Measurement in Aquaculture [*]

Authors: Hailen Andrea Chacón López,

Natalia Estefanía Cruz Castillo,

Jose Luis Parra Villamizar [**]

Keywords: Dissolved oxygen, optoelectronic sensor, absorption spectroscopy, aquaculture, Internet of Things (IoT), multiple linear regression (MLR), water quality monitoring.

Description:

Aquaculture systems require continuous monitoring of dissolved oxygen to ensure the survival and productivity of cultivated species; however, commercially available sensors present high costs and limited accessibility for small-scale producers. This work presents the design and implementation of a low-cost optoelectronic sensor for the estimation of dissolved oxygen in water. The system uses a light source, a multispectral sensor, and complementary variables such as temperature and pressure, from which optical signals are acquired under real experimental conditions. These signals are processed using the absorbance equation to relate the measured optical intensity to the properties of the aqueous medium. The resulting variables are used as inputs to a supervised learning model that relates the measurements to reference values obtained using a commercial dissolved oxygen sensor. System performance was evaluated using a dataset divided into training (70%) and testing (30%) subsets obtained under real measurement conditions, achieving a coefficient of determination of $R^2 = 0.9582$ and a root mean squared error of $RMSE = 0.3801$ mg/L during offline evaluation. Additionally, the system integrates a real-time visualization platform based on Grafana, enabling continuous monitoring of the measured variables. The proposed system represents an accessible and scalable alternative for water quality monitoring, with the potential to contribute to the optimization of productive processes in small- and medium-scale aquaculture systems.

---

[*] BSc Thesis

[**] Faculty of Physical-Mechanical Engineering. School of Electrical, Electronic and Telecommunications Engineering. Director: Rodolfo Villamizar Mejía. Doctor. Codirector: Omar Javier Tijaro Rojas. Doctor.

Introduction

In 2021, global consumption of aquatic foods of animal origin reached 162.5 million tons, with an average annual growth of 3.0% since 1961 (Food and Agriculture Organization of the United Nations, 2024). This increase has been driven by the development of strategies aimed at improving community nutrition and strengthening food security (Food and Agriculture Organization of the United Nations, 2002). Currently, aquaculture surpasses capture fisheries in terms of aquatic animal production; however, this sector is concentrated in a limited number of countries that generate more than 89.8% of the total production. A common characteristic among them is their focus on technological innovation, which includes technology transfer, the strengthening of technical capacities, and the adoption of new productive solutions (Food and Agriculture Organization of the United Nations, 2024).

Despite its strategic relevance, the National Plan for the Development of Sustainable Aquaculture in Colombia shows significant weaknesses in the technology transfer system. In particular, research and human resource training mechanisms fail to effectively impact producers with limited resources, restricting the adoption of innovations that could improve the efficiency and sustainability of their production systems (Autoridad Nacional de Acuicultura y Pesca, 2013).

Among the critical processes in aquaculture is the continuous monitoring of physicochemical water parameters, whose lack of control can severely affect the health of cultivated species and even cause their mortality. Among these parameters, dissolved oxygen is one of the most relevant, as it directly participates in the metabolic processes of aquatic organisms. Although there are commercial systems capable of measuring this variable with high precision, their costs are usually high, limiting their adoption by small and medium-scale producers. As a result, numerous culture systems are managed without precise and real-time information, which increases the risk of production losses, disproportionately impacting smaller producers with economic limitations.

The sensors most commonly used for this measurement are polarographic and galvanic sensors, based on electrical currents generated by electrochemical reactions. Although they

provide reliable results, with typical accuracy levels between ±1% and ±3% of the reading under controlled conditions, they present limitations associated with frequent maintenance, prolonged stabilization times, and susceptibility to chemical interferences. Optical sensors, in contrast, use variations in the light signal to determine the concentration of dissolved oxygen. Since they do not rely on electrochemical processes, they eliminate problems such as electrolyte consumption, continuous polarization, and accelerated degradation of internal components (Hamilton Company, n.d.), making them a more stable and lower-maintenance alternative for continuous monitoring.

Within this framework, the present work proposes the design and development of a low-cost optoelectronic sensor for dissolved oxygen measurement, aimed at small and medium-scale producers in aquaculture systems. Unlike currently available commercial optical sensors, whose price limits their widespread implementation, this development prioritizes affordability and scalability without sacrificing measurement reliability, integrating low-cost components with calibration techniques adapted to the Colombian productive context.

As a result of this work, a functional prototype capable of acquiring and proce-ssing optical signals related to dissolved oxygen was developed. In offline analysis and model training using experimental data in Python, the proposed regression approach showed good performance in estimating dissolved oxygen within aquaculture-relevant ranges.

However, during real-time deployment, discrepancies were observed between the model outputs and expected physical behavior, indicating limitations in generalization under dynamic operating conditions. These results highlight that, although the system demonstrates strong potential in controlled experimental settings, further work is required to improve model robustness and adaptability in real-world environments.

Despite these limitations, the proposed system provides a low-cost platform for water quality monitoring and establishes a foundation for future improvements in data acquisition, modeling, and real-time inference strategies.

1. Objectives

1.1 General Objective

Design, implement, and validate a low-cost optoelectronic sensor based on absorption spectroscopy for the indirect, real-time measurement of dissolved oxygen in aquaculture systems, ensuring precision, affordability, and ease of use.

1.2 Specific Objectives

Investigate and analyze recent advances in optoelectronic sensors for dissolved oxygen measurement, with emphasis on absorption spectroscopy-based technologies, to provide a foundation for the design of the proposed sensor.

Define the technical requirements and specific design conditions necessary for the sensor to operate in aquaculture environments, considering environmental factors such as temperature, salinity, and potential sources of interference.

Design and implement a functional prototype of the optoelectronic sensor that meets the established requirements for aquaculture applications.

Validate the sensor's performance through experimental tests conducted under controlled conditions in order to evaluate its accuracy, reliability, and effectiveness in measuring dissolved oxygen.

2. Body of the thesis

In this chapter, the theoretical foundations that support the development of the dissolved oxygen measurement system are presented. Its importance in aquaculture, the measurement principles, and the technological tools used for data acquisition and processing are addressed, which constitute the conceptual basis of the proposed system.

2.1 Dissolved oxygen

Dissolved oxygen (DO) corresponds to the gaseous oxygen present in water, incorporated mainly through exchange with the atmosphere and the movement or agitation of water. It is available to aquatic organisms, being essential for their survival and proper growth. Likewise, it constitutes a key indicator of water quality, making its monitoring indispensable in aquaculture systems (Recalde Mórtola, 2022).

Dissolved oxygen is commonly expressed as the concentration of oxygen present in water, measured in mg/L. Its value is not constant, as it depends on various physical, chemical, and biological variables present in the aquatic environment (Junta Regional del Control de Calidad de Agua, n.d.).

2.1.1 Factors Affecting Dissolved Oxygen

The concentration of dissolved oxygen in water bodies is not constant, but depends on various physical, chemical, and biological factors, such as:

- Temperature: oxygen solubility decreases as water temperature increases, therefore DO is higher in cold water and lower in warm water (U.S. Geological Survey, 2018).
- Movement and aeration: water movement favors gaseous exchange with the atmosphere, increasing DO (Recalde Mórtola, 2022).
- Organic matter: the decomposition of organic matter increases oxygen consumption by microorganisms, reducing its concentration in water (U.S. Geological Survey, 2018).
- Barometric pressure: oxygen solubility decreases with atmospheric pressure; therefore, at higher altitudes, lower DO concentrations occur.

- Salinity: increased salinity reduces oxygen solubility, decreasing DO concentration under similar temperature and pressure conditions (GLOBE Program, 2005).

2.1.2 Optimal dissolved oxygen ranges in aquaculture

Dissolved oxygen presents optimal ranges for proper development in aquaculture, which vary according to the species. Levels below these ranges can cause mortality, growth reduction, and alterations in embryonic and larval stages (Junta Regional del Control de Calidad de Agua, n.d.). Table 1 summarizes the critical and optimal ranges of dissolved oxygen and temperature for some species of interest in Colombia.

Table 1

Temperature and DO ranges for cultured species in Colombia

Species	DO (mg/L)	Temperature (°C)
 Red Tilapia	Critical: <3 Optimal: 3–5	Critical: <20 / >34 Optimal: 25–30
 Trout	Critical: <5 Optimal: 5–7	Critical: <1 / >22 Optimal: 15–17
 Shrimp	Critical: <3 Optimal: >4	Critical: <28 / >33 Optimal: 28–30

Note. Ranges and thresholds compiled from Agroguajira (n.d.), Colprecios (2026), Food and Agriculture Organization of the United Nations (n.d.), Laowisit (2021), PriceSmart (2025), and Skretting (s.f.-a, s.f.-b).

2.2 Dissolved oxygen measurement methods

Among the main methods used for dissolved oxygen (DO) measurement are the Winkler method, colorimetry, absorption spectroscopy, electrochemical methods, and optical methods based on fluorescence quenching (Zhang et al., 2024).

2.2.1 Winkler method

The Winkler method is a chemical technique based on redox reactions that allow determining the concentration of dissolved oxygen through titration. Although it presents high precision, it requires multiple reagents and is not suitable for real-time measurements (Recalde Mórtola, 2022).

2.2.2 Electrochemical method

The electrochemical method measures dissolved oxygen from the current generated by redox reactions in electrodes. Although it is widely used and reliable, it presents oxygen consumption during measurement and requires periodic maintenance and calibration (Wei et al., 2019).

2.2.3 Optical method

Optical methods are based on the interaction between electromagnetic radiation and matter, where the absorption of light energy induces electronic transitions from the ground state to excited states.

- Fluorescence quenching: Fluorescence occurs when an excited molecule emits a photon as it returns to its ground state. The presence of dissolved oxygen reduces the intensity or lifetime of this signal through quenching (De Gerónimo & Falomir Lockhart, 2022).

  This relationship is described by the Stern–Volmer equation, as shown in equation 1:

$$\frac{I_0}{I} = \frac{\tau_0}{\tau} = 1 + K_{SV}[O_2] \tag{1}$$

  where I_0 and I are the fluorescence intensities without and with oxygen, τ_0 and τ are the lifetimes, and K_{SV} is the Stern–Volmer constant.

- Colorimetry and spectrophotometry: These are optical techniques that allow determining the concentration of a substance from light absorption. Colorimetry measures at a specific wavelength, while spectrophotometry analyzes a range of wavelengths.

  When a light beam strikes the sample, part of the radiation is absorbed, reducing the transmitted intensity. This phenomenon is quantified through absorbance, as shown in

equation 2:

$$A = -\log_{10}\left(\frac{I_0}{I}\right) \tag{2}$$

Absorbance is related to concentration through the Beer–Lambert law, presented in equation 3:

$$A = \varepsilon bc \tag{3}$$

where ε is the molar absorption coefficient, b is the optical path length, and c is the analyte concentration (Zhang et al., 2024).

In order to compare the main dissolved oxygen measurement techniques, Table 2 summarizes their characteristics in terms of cost, accuracy, maintenance, and measurement method.

Table 2

Comparison of dissolved oxygen measurement methods

Sensor type	Cost	Accuracy	Maintenance	Measurement method
Polarographic (Clark type)	Low to moderate	±0.1–0.3 mg/L	High: regular calibration; membrane and electrolyte replacement	Electrochemical
Galvanic	Low to moderate	±0.1–0.3 mg/L	Moderate: less frequent than Clark type	Electrochemical
Luminescent	High	±0.05–0.1 mg/L	Low: minimal calibration; robust design	Optical
Winkler	Low	High (±0.01–0.05 mg/L)	High: chemical handling and manual procedures	Winkler

Note. Adapted from Desun Uniwill (2025).

2.3 Internal photoelectric effect of the AS7265x sensor

The AS7265x spectroscopy sensor is composed of three devices (AS72651, AS72652, and AS72653), which integrate photodiode arrays using CMOS technology. Each one incor-

porates nano-optical interference filters with an approximately Gaussian response and a bandwidth (FWHM) of 20 nm, as shown in Figure **??**.

Figure 1

Spectral response of the 18 channels of the AS7265x sensor

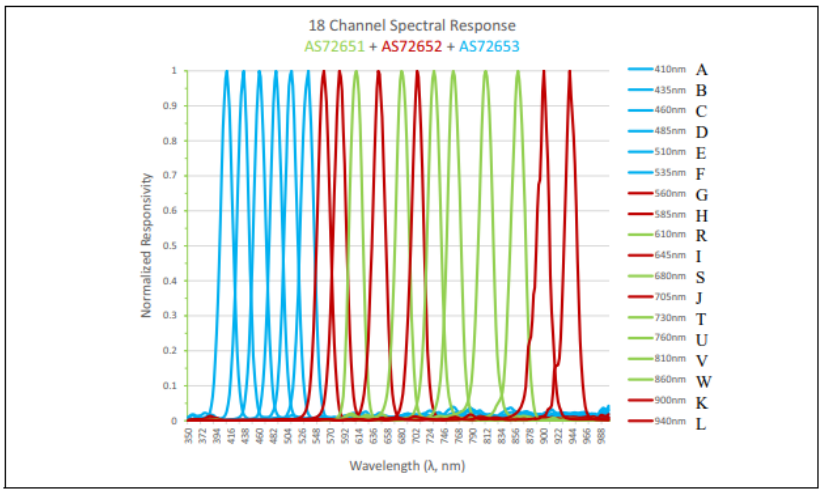

Note. Spectral distribution adapted from ams AG (2018b).

The operation of multispectral sensors such as the AS7265x can be described through a block diagram, in which the stages of optical radiation capture, signal conversion, and digital data acquisition are represented. Figure 2 presents a representation of this process.

Figure 2

Block diagram of the internal operation of the AS7265x sensor

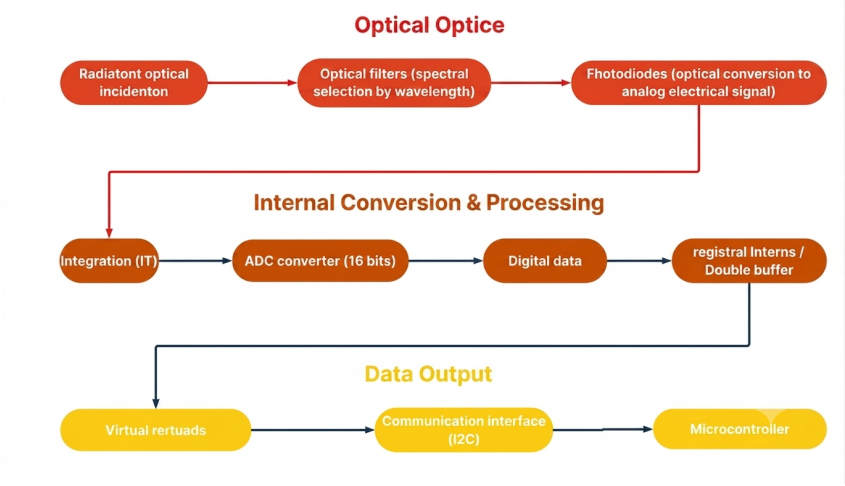

Note. Internal blocks and signal routing architecture adapted from ams AG (2018b).

2.4 Performance parameters for DO measurement

Performance parameters allow evaluating the metrological characteristics of the measurement system, such as its measurement capability, accuracy, and consistency (Joint Committee for Guides in Metrology, 2008; Taylor, 1997).

- Measurement range: It is defined as the interval $[OD_{\min}, OD_{\max}]$ within which the measurement system guarantees adequate performance in terms of accuracy and repeatability.

- Accuracy: It is evaluated through the absolute error and the relative error with respect to the reference sensor. The absolute error is calculated as shown in equation 4, while the relative error is obtained through equation 5:

$$E_a = |OD_{sensor} - OD_{reference}| \tag{4}$$

$$E_r = \frac{|OD_{sensor} - OD_{reference}|}{OD_{reference}} \times 100 \tag{5}$$

- Precision: It indicates the closeness between repeated measurements and is evaluated through the standard deviation, which is calculated according to equation 6:

$$\sigma = \sqrt{\frac{\sum_{i=1}^{n}(x_i - \bar{x})^2}{n-1}} \tag{6}$$

- Repeatability: It is defined as the ability of the system to obtain consistent results under the same experimental conditions, evaluated through the standard deviation of a set of measurements performed under identical conditions.

- Linearity: It is determined from the coefficient of determination of the calibration curve, whose calculation is presented in equation 7:

$$R^2 = 1 - \frac{\sum(y_i - \hat{y}_i)^2}{\sum(y_i - \bar{y})^2} \tag{7}$$

- Resolution: It corresponds to the minimum detectable variation in the dissolved oxygen concentration. This is determined from the relationship between the minimum detectable variation of the signal and the slope of the calibration curve, as shown in equation 8:

$$Resolution_{OD} = \frac{\Delta I}{|a|} \tag{8}$$

where ΔI is the minimum variation in the sensor signal and a corresponds to the slope of the calibration curve.

2.5 Multiple linear regression

Multiple linear regression is a statistical model that allows establishing a linear relationship between a dependent variable and multiple independent variables. This model assumes that the output variable can be expressed as a linear combination of the input variables, together with an error term (Montgomery et al., 2012).

Mathematically, this model is expressed as shown in equation 9:

$$y = \beta_0 + \beta_1 x_1 + \beta_2 x_2 + \cdots + \beta_n x_n + \varepsilon \tag{9}$$

where y represents the dependent variable, x_i correspond to the independent variables, β_i are the model coefficients, and ε is the random error term.

2.6 Model evaluation metrics

Model evaluation metrics allow quantifying the performance of the estimation algorithm in terms of precision, goodness of fit, and stability with respect to experimental data (Hastie et al., 2009; Montgomery et al., 2012).

- Mean Squared Error (MSE): It measures the average of the squared errors between the real and estimated values, penalizing larger errors to a greater extent. This indicator is calculated as shown in equation 10:

$$MSE = \frac{1}{n}\sum_{i=1}^{n}(y_i - \hat{y}_i)^2 \tag{10}$$

- Root Mean Squared Error (RMSE): It corresponds to the square root of the mean squared error defined in equation 10, and is expressed in the same units as the output variable, facilitating its interpretation. Its calculation is presented in equation 11:

$$RMSE = \sqrt{\frac{1}{n}\sum_{i=1}^{n}(y_i - \hat{y}_i)^2} \tag{11}$$

- Coefficient of determination (R^2): It indicates the proportion of the variability of the data that is explained by the model. Values close to 1 indicate a better fit. Its calculation is presented in equation 12:

$$R^2 = 1 - \frac{\sum_{i=1}^{n}(y_i - \hat{y}_i)^2}{\sum_{i=1}^{n}(y_i - \bar{y})^2} \tag{12}$$

2.7 IoT tools

The Internet of Things (IoT) enables the interconnection of physical objects through communication networks, in order to exchange information and integrate the physical world with the digital one (Atzori et al., 2010). In this context, devices can connect to the Internet, interact with their environment, collect data, and transmit them for processing, enabling remote monitoring and control of various processes.

An IoT system is composed of different functional levels, which include data acquisition through sensors, local processing through embedded devices, information transmission through communication protocols, and storage on specialized platforms (Gubbi et al., 2013). These systems have been established as a fundamental tool for monitoring environmental variables, especially in contexts that require continuous data acquisition.

Tools such as Node-RED facilitate the integration of data flows through graphical interfaces, while time-series-oriented databases such as InfluxDB allow storing information associated with temporal references. Additionally, platforms such as Grafana enable real-time data visualization through interactive dashboards, facilitating their interpretation.

2.8 Literature Review

The development of sensors for measuring dissolved oxygen (DO) has evolved significantly in recent years, especially with the incorporation of optoelectronic technologies that enable indirect and, in some cases, non-contact measurements. These technologies have been widely investigated due to their potential to improve accuracy, reduce costs, and facilitate implementation in aquaculture systems.

One of the earliest relevant approaches was presented by (Li et al., 2015), who developed a fluorescence-based sensor. This work introduced the use of oxygen-sensitive luminescent compounds, enabling real-time measurements. However, the system required direct contact with the aquatic medium, which implied operational and maintenance limitations.

In another line of research, (Silva et al., 2016) developed sensors using chlorophyll-derived complexes, offering a more sustainable alternative to traditional materials based on transition metals. This approach demonstrated a high correlation in DO measurement, highlighting the potential of biological materials in optoelectronic sensors.

More recently, (Miura et al., 2021) investigated absorption spectroscopy in the ultraviolet region, establishing a strong relationship between absorbance and dissolved oxygen concentration. Nevertheless, this method presents limitations related to the high cost of the equipment and the risks associated with UV radiation.

As an evolution of these approaches, (Tran et al., 2024a) proposed the use of spectroscopy in the visible and infrared regions, enabling non-contact measurements with lower cost and greater safety. In addition, this work incorporates rigorous statistical analysis to validate the results against commercial sensors, making it a key reference for the development of practical and accessible solutions.

Complementarily, recent literature shows a growing trend toward the integration of IoT technologies into water quality monitoring systems. In this context, platforms have been developed that combine dissolved oxygen, temperature, and pH sensors with wireless transmission systems and cloud storage, enabling real-time remote monitoring (Medina et al., 2022). Likewise, other studies have implemented solutions based on microcontrollers and Wi-Fi connectivity for data acquisition and visualization in aquaculture applications, demonstrating the

potential of IoT to improve information management and decision-making processes in these systems (Suárez et al., 2024).

Based on this review, a clear trend can be identified toward the development of non-invasive, low-cost solutions with continuous monitoring capabilities. In this context, the approach based on visible and infrared spectroscopy proposed by (Tran et al., 2024a), together with the integration of IoT technologies, emerges as a suitable alternative for the development of dissolved oxygen measurement systems that are accessible, scalable, and applicable in real-world aquaculture environments.

2.9 Solution design

In order to describe the general architecture of the proposed system, a block diagram is presented that illustrates the interaction between the different modules that make up the prototype, as shown in Figure 3. This includes the multispectral acquisition stage, based on the AS7265x sensor, together with the measurement of complementary variables such as temperature and barometric pressure; the local processing of information through the ESP32 microcontroller; the wireless transmission of data through the MQTT protocol; as well as its storage in an InfluxDB database and its subsequent real-time visualization through Grafana.

Figure 3

Block diagram of the general architecture of the proposed system

Note. Overview of the hardware integration, signal conditioning stages, and data flow layers.

2.9.1 Conceptual design

Based on what was reported by Tran et al. (2024b), the present project was proposed around the use of absorption spectroscopy as an optical alternative for dissolved oxygen measurement, in contrast to techniques based on fluorescence emission. This approach takes advantage of the interaction between electromagnetic radiation and the water sample to infer the dissolved oxygen concentration from variations in absorbance. For this purpose, a multispectral approach is employed using the AS7265x sensor, which allows acquiring information at different wavelengths of the visible and near-infrared spectrum, facilitating the capture of more complete spectral signatures of the sample.

The main variable of the system is the dissolved oxygen concentration (DO). Additionally, this work considers including complementary variables such as temperature and barometric pressure, due to their influence on oxygen solubility and measurement conditions. The inclusion of these variables allows improving the accuracy in DO estimation by considering environmental factors that affect system behavior. Based on these principles, a structure was designed that allows controlled interaction between optical radiation and the water sample.

2.9.2 Mechanical design

The prototype was designed with a compact structure that integrates the electronic and optical components into a main body. This includes an internal channel that allows controlled circulation of the water sample, facilitating its interaction with the measurement elements.

The AS7265x multispectral sensor was placed in direct proximity to the measurement chamber, ensuring proper acquisition of the optical signal. Complementarily, an illumination source based on a light-emitting diode (LED) was integrated, responsible for providing incident radiation on the sample under controlled conditions. The approximate distance between the illumination source and the sensor was established at 5 cm, defining the optical path through the sample. Likewise, the temperature (DS18B20) and pressure (BMP280) sensors were positioned at representative points of the system, allowing the capture of environmental variables relevant to dissolved oxygen estimation. As shown in Figure 4, the distribution of the main components includes the multispectral sensor, the illumination source, and auxiliary sensors.

Figure 4

Front view of the prototype showing the location of its main components

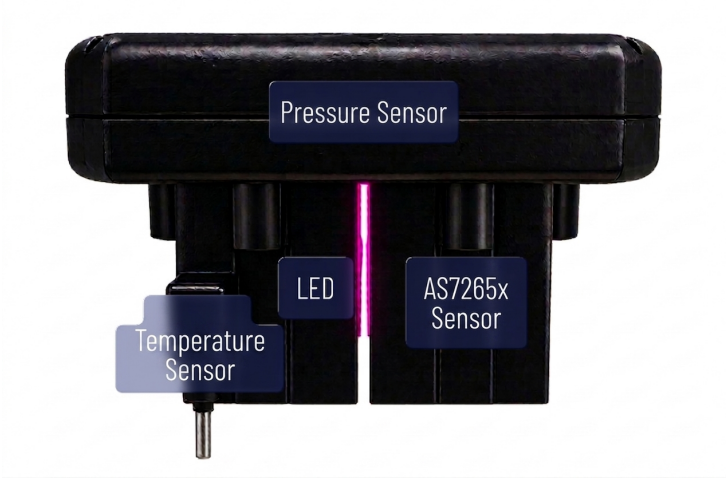

Note. Spatial distribution and structural housing layout designed for the optoelectronic acquisition modules.

Material selection was carried out considering criteria such as mechanical resistance, compatibility with the aqueous environment, and ease of manufacturing. The structure was designed using three-dimensional modeling tools and manufactured through 3D printing using PETG filament. Additionally, an epoxy resin coating was applied as a barrier against fluid leakage, together with sealing elements that guarantee system watertightness during operation. The STL files corresponding to the sealing elements and structural mechanical parts of the prototype are provided in Chapter 2.15, specifically in Appendix F.

In terms of operation, the prototype was conceived so that its lower section remains submerged, allowing direct interaction with the water sample. Meanwhile, the power and electronic conditioning stage is placed in the upper section, isolated from fluid contact, in order to protect the electronic components.

2.9.3 Electronic design

The electronic system of the prototype was designed to integrate the functions of data acquisition, processing, power supply, and illumination source control, necessary for the estimation of dissolved oxygen from multispectral information.

In Table 3, the components used and their respective functions within the proposed architecture are presented. The schematic circuit and PCB design of the system are presented

in Chapter 2.15, specifically in Annexes B.

Table 3

Components of the proposed system

Component	Function
AS7265x	Multiband spectral measurement
DS18B20	Thermal compensation of the system
BMP280	Barometric compensation in the measurement
ESP32	Processing and system management
IRFZ44N	Switching and control of the LED
Power Bank	Autonomous power supply
Resistors	Current limiting and biasing
Pull-up resistors	Stabilization of communication lines

2.9.4 Acquisition stage

Data acquisition is performed using the AS7265x multispectral sensor, which communicates with the central unit through the I^2C bus. Complementarily, the DS18B20 and BMP280 sensors enable the measurement of temperature and pressure, respectively, providing variables necessary for the compensation of dissolved oxygen estimation.

2.9.5 Processing stage

Information processing is carried out by the ESP32 microcontroller, which manages sensor reading, illumination source control, and data communication. Interaction with the devices is performed mainly through digital protocols such as I^2C, enabling efficient integration of the different modules of the system.

2.9.6 Power supply and power control

The system is powered by a portable power bank source, providing autonomy during operation. For illumination source control, a driver for a 1 W LED based on an IRFZ44N MOSFET was implemented, configured as a switch and controlled by the ESP32.

The design incorporates a 6.8 Ω resistor in series with the LED for current limiting, a 10 kΩ resistor at the gate in pull-down configuration to avoid undesired activations, and a 220 Ω resistor in series with the gate to mitigate transients and protect the microcontroller outputs.

2.9.7 Autonomy

To estimate system autonomy, an analysis of the energy consumption of each active component of the prototype was performed. The ESP32, operating with active WiFi connectivity, presents a typical consumption of approximately 200 mA according to manufacturer specifications (Espressif Systems, 2023).

The active LED driver, powered from the 5 V pin of the ESP32 through a $6{,}8\,\Omega$ limiting resistor and a 1 W LED with a voltage drop of $3{,}2\,V$, operates with a current calculated using Ohm's Law, as shown in equation 13:

$$I_{LED} = \frac{V_{cc} - V_{LED}}{R} = \frac{5{,}0 - 3{,}2}{6{,}8} \approx 265\,\text{mA} \tag{13}$$

The AS7265x spectral sensor, composed of the three chips AS72651, AS72652 and AS72653, presents a typical consumption of approximately 5 mA under normal operating conditions, according to its datasheet (ams AG, 2018a).

The BMP280 and DS18B20 sensors contribute approximately 3 mA and 2 mA respectively, values estimated from their electrical characteristics specified by the manufacturers (Bosch Sensortec, 2018; Maxim Integrated, 2019), resulting in an estimated total system consumption, as expressed in equation 14:

$$I_{\text{total}} = 200 + 265 + 5 + 3 + 2 = 475\,\text{mA} \tag{14}$$

The power supply used is a portable battery of 10,000 mAh. Considering a typical internal conversion efficiency of 85% for this type of device, the available effective capacity is estimated at 8500 mAh.

The estimated system autonomy is calculated from the relationship between electrical capacity and consumed current, as shown in equation 15:

$$t = \frac{C_{\text{effective}}}{I_{\text{total}}} = \frac{8500\,\text{mAh}}{475\,\text{mA}} \approx 17{,}9\,\text{hours} \tag{15}$$

This result indicates that the prototype can operate continuously for approximately 18 hours with a single charge, which is sufficient to cover a full field monitoring session.

2.9.8 Communication and software system

The system was structured as a continuous flow of acquisition, transmission, storage, and data processing, divided into two phases: calibration and operation. During the calibration phase, experimental data were acquired using an ESP32, responsible for reading the multi-spectral sensor and the temperature and pressure sensors. The acquisition was performed at a frequency of 1 Hz, allowing the capture of system dynamics and the formation of a suitable dataset for model training.

The general flow of acquisition, processing, and estimation is presented in Figure 5.

Figure 5

System workflow of the proposed monitoring platform

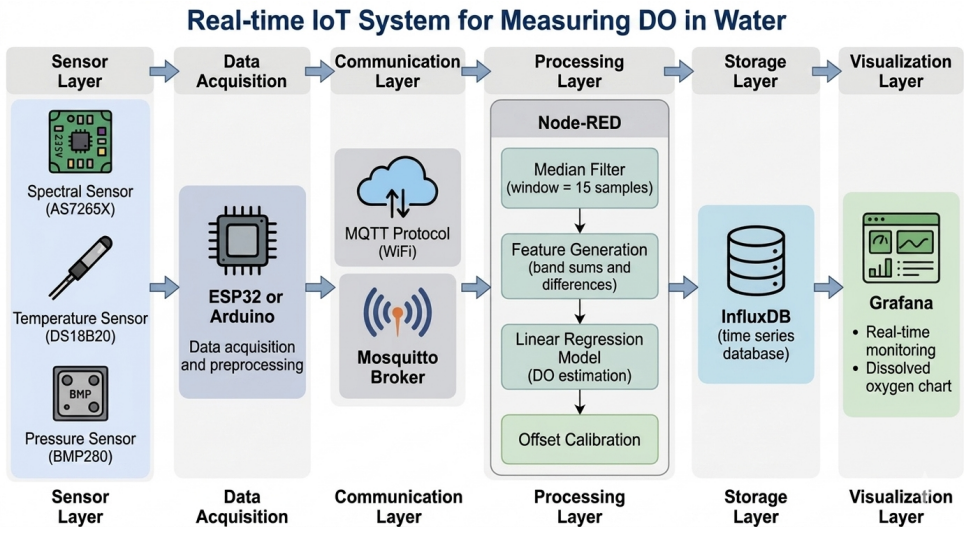

Note. Sequential execution path showing sensor initialization, barometric and thermal compensation loops, and predictive model output generation.

2.9.9 MQTT protocol

Data transmission was performed wirelessly using the MQTT protocol, which enables efficient communication under the publisher–subscriber model. This choice is based on its low resource consumption, low latency, and ease of integration with processing platforms such as Node-RED.

The acquired data were sent in JSON format through the Wi-Fi network to the processing environment, enabling real-time data management.

2.9.10 Data storage and processing

In the Node-RED environment, the received data were subjected to a preprocessing stage aimed at improving their quality and consistency. For this purpose, a temporary storage mechanism based on a fixed-size buffer was implemented, in which consecutive samples were grouped. Once the defined number of samples was reached, a filtering process was applied through the removal of extreme values and the calculation of the median, reducing the effect of noise in the measurements.

Subsequently, the information was stored in a time-series database (InfluxDB) using a structure based on independent measurements and tags, which facilitates querying, analysis, and differentiation between experiments. At this stage, reference measurements obtained using a reference sensor (FDO 1100 IDS) (SI Analytics GmbH, 2014) were also integrated.

2.9.11 Visualization dashboard (Grafana)

The stored data were visualized using the Grafana platform, enabling real-time monitoring of the acquired variables, including spectral response, temperature, pressure, and dissolved oxygen estimation. This tool facilitates the interpretation of system behavior and continuous monitoring during operation.

Once the calibration phase was completed, the model was trained and integrated into the system, initiating the operation phase, in which the prototype estimates dissolved oxygen concentration from spectral variables.

The codes developed for acquisition, processing, and visualization of the system are available in the annex section of this document, specifically in Chapter 2.15, Annex A, where the experimental data and system demonstration are presented.

2.10 Results

2.10.1 Experimental protocol

During the experimental stage, it was necessary to reduce the dissolved oxygen in the water to values close to zero in order to cover the entire dynamic range of the sensor. For this purpose, a reducing solution based on sodium bisulfite ($NaHSO_3$) was prepared, due to its ability to consume oxygen.

The solution was prepared by dissolving approximately 30 g of sodium bisulfite in 1 L

of water, using manual agitation until complete dissolution. During the measurements, the sensor was temporarily removed from the main container, approximately 30 mL of the solution were added, and homogenization was allowed to occur.

The effect of the bisulfite occurs progressively, allowing a controlled decrease in dissolved oxygen. In the experimental scenario, the decrease from saturation levels to values close to the minimum measurable level took approximately 2 h. In cases where the concentration stabilized and did not continue decreasing, an additional amount of the bisulfite solution was added to reactivate the process.

In order to guarantee traceability and reproducibility of the experimental procedure, evidence of the measurement process is included in the project annexes, such as experimental records, acquired data, and audiovisual material from the test development. This information can be consulted in Chapter 2.15, specifically in Annexes C and D, corresponding to the experimental data and system demonstration.

2.10.2 System modeling

The objective of this stage was to establish a relationship between the measured spectral variables and the dissolved oxygen concentration obtained using the FDO 1100 IDS sensor. For this purpose, two types of data were used: measurements taken in vacuum conditions, that is, outside the water, in order to determine the intensity perceived by the sensor in air, and measurements performed within the aqueous medium.

From these data, absorbance was calculated using Equation 2. Subsequently, the data were preprocessed through cleaning stages, conversion to numerical format, removal of incomplete records, and the application of smoothing using a moving average.

Once preprocessing was completed, the dataset was divided into 70% for training and 30% for validation. Using the training dataset, a multiple linear regression (MLR) model with Ridge regularization was implemented, whose coefficients are presented in Table 4 and whose formulation is described in Equation 9. Subsequently, the model was evaluated using the validation dataset to analyze its generalization capability.

Additionally, an extra validation was performed using independent data that were not part of the original training and validation dataset. During this stage, the experimental condi-

tions presented variations compared to those used during training, particularly in the concentration of the reducing agent (sodium bisulfite) and in the system temperature, which allowed evaluating the model behavior under conditions different from the initial ones.

During validation under modified conditions, a decrease in model performance was observed, mainly attributed to variations in the concentration of sodium bisulfite and system temperature. These variations affected the reproducibility of the physicochemical conditions used during training.

Table 4

Coefficients of the dissolved oxygen estimation model

Variable	Coefficient	Variable	Coefficient
Intercept	-153.094665	J	-34.459862
A	54.456093	K	-75.531055
B	45.995892	L	-47.828787
C	7.356419	R	-5.097996
D	-9.479781	S	35.537653
E	-91.757680	T	17.659857
F	-46.169887	U	1.676931
G	-7.949178	V	-54.103327
H	114.865328	W	-86.220842
I	-81.860957	TempDS	-7.376161
Pressure	0.375384		

Note. Numerical parameters extracted directly from the weights of the finalized linear regression architecture.

The results are presented in Table 5, where metrics such as R^2, RMSE, and MSE obtained from the validation dataset (30%) are compared, allowing analysis of the impact of variable selection and smoothing on model accuracy.

Table 5

Comparative evaluation of models for DO estimation

Model	**No. Variables**	R^2	**RMSE**	**MSE**
All bands (without smoothing)	18	0.93	0.47	0.22
All bands (median 15)	18	0.95	0.38	0.14
Band selection (without smoothing)	6	0.91	0.53	0.28
Band selection (median 15)	6	0.94	0.45	0.28

Note. Performance metrics evaluated across different spectral channel configurations and signal filtering stages.

From the results presented in Table 5, it is observed that filtering using a median with a window of 15 samples improves model performance, evidenced by a higher R^2 and a reduction in RMSE and MSE. This is due to its robustness against outliers, allowing more representative signals to be obtained and reducing the influence of noise.

Likewise, the use of all spectral bands shows the best overall performance, indicating that relevant information for dissolved oxygen estimation is distributed throughout the spectrum.

The comparison between measured dissolved oxygen values and those estimated by the model is presented in Figure 6.

Figure 6

Comparison between measured dissolved oxygen and model-estimated dissolved oxygen

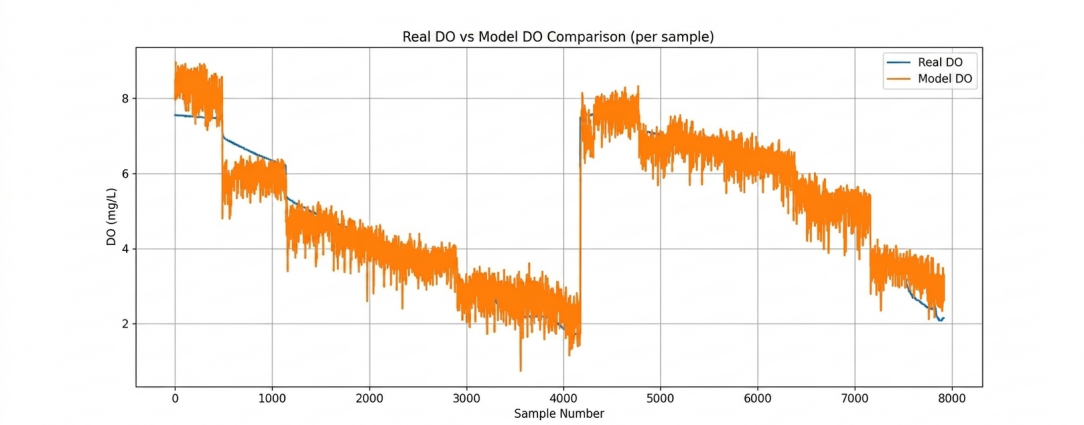

Note. Time-series validation behavior contrasting the reference sensor readings against the algorithmic predictions across the evaluation dataset.

Additionally, Figure 7 presents a scatter plot between the real and estimated dissolved oxygen values. In this graph, the distribution of data around the identity line can be observed, allowing visualization of the relationship between both variables and the general behavior of the model.

Figure 7

Scatter plot of measured versus model-estimated dissolved oxygen

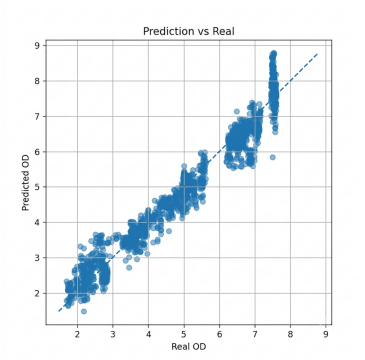

Note. Distribution profile indicating the goodness-of-fit and dispersion trajectory between reference measurements and predicted values across the testing dataset.

The results of the metrological performance of the system are presented in Table 6, where parameters such as measurement range, absolute and relative errors, precision, and resolution are summarized. These indicators allow evaluating the accuracy and stability of the

system in dissolved oxygen estimation under the considered experimental conditions.

Table 6

Performance parameters of the DO measurement system

Parameter	Value	Unit
Measurement range	1.7 – 7.6	mg/L
Absolute error	0.2897	mg/L
Relative error	6.8390	%
Precision (std. deviation)	0.3800	mg/L
Linearity (R^2)	0.9582	–
Resolution	0.0100	mg/L

Note. Metrics derived from laboratory calibration and validation routines against an industrial optical reference probe.

Once the model was selected, it was implemented in the prototype for real-time operation. For this purpose, median filtering was applied over windows of 15 samples, from which the prediction was generated. Dissolved oxygen estimation was performed as a function of the light intensities measured at different wavelengths, additionally incorporating temperature and pressure compensation.

2.10.3 Data visualization

Data visualization was performed using the Grafana platform, integrated with the InfluxDB database for real-time monitoring of system variables. As shown in Figure 8, an interactive panel was implemented that displays the temporal evolution of the estimated dissolved oxygen concentration, along with its instantaneous value through numerical indicators and gauge-type charts.

The panel includes complementary variables such as system temperature and spectral signals at different wavelengths, allowing a more detailed analysis of sensor behavior. The configuration was based on Flux-type queries with temporal aggregation windows, facilitating noise reduction, trend interpretation, and continuous monitoring of system performance.

Figure 8

Grafana visualization of dissolved oxygen estimation in a water sample under initial conditions

Note. Real-time telemetry dashboard display tracking stability, algorithmic DO prediction curves, and sensor response under baseline laboratory testing.

A reference mechanism based on dissolved oxygen saturation concentration was implemented, which represents the DO value corresponding to 100% saturation as a function of temperature and atmospheric pressure. This approach allows dynamically adjusting the model estimation considering environmental conditions in real time.

The saturation concentration is calculated using an empirical expression dependent on temperature and pressure, as shown in Equation 16:

$$OD_{sat} = \left(14.652 - 0.41022T + 0.007991T^2 - 0.000077774T^3\right) \cdot \frac{P}{101.325} \tag{16}$$

where T is the temperature in °C, P is the atmospheric pressure in kPa, and OD_{sat} is the dissolved oxygen concentration under saturation conditions expressed in mg/L (Super Global Calculator, 2024).

2.11 Limitations of the prototype design and implementation

During the testing stage, several limitations associated with the design, manufacturing, and experimental validation of the prototype were identified, which are summarized below:

- System watertightness: Leakage problems occurred at the optical interfaces (lenses) and at the cable gland, associated with hydrostatic pressure under immersion conditions, which caused water to enter the interior of the device.

- Manufacturing conditions: The presence of support material not removed in critical zones of the manufacturing process was identified, affecting fastening points and reducing the effective fastening elements from four to two.

- Mechanical stability: The incorporation of a portable battery in the upper part of the system modified the mass distribution, shifting the center of gravity above the center of buoyancy. This generated instability during operation, increasing the risk of tipping.

- Experimental DO control: Difficulties were encountered in regulating dissolved oxygen concentration using sodium bisulfite, due to the non-linear relationship between the added amount and the resulting concentration. For this reason, the use of a reference sensor was necessary to guarantee measurement reliability.

- Data variability: The implementation of real-time normalization techniques was restricted by the availability of experimental data, which were acquired mostly under a single temperature condition. This lack of thermal variability limits model generalization under temperature changes, reducing system robustness in scenarios different from the training conditions.

- Model capacity: Although the use of more complex models, such as MLP-type neural networks, was considered, the processing platform used (Node-RED) does not provide adequate support for real-time implementation. Consequently, a multiple linear regression (MLR) model was selected, prioritizing computational feasibility over model complexity.

2.12 Improvement strategies implemented

In order to mitigate leakage problems, it was decided to permanently fix the optical elements and reinforce the seals, prioritizing hermetic sealing over design modularity.

Regarding manufacturing issues, it was verified that, despite the reduction in fastening points, the resulting attachment was sufficient to guarantee component stability during operation, allowing the continuation of development without requiring an immediate redesign.

To address stability problems, a float was designed and incorporated as a stabilizing element, increasing the restoring moment of the system and promoting its balance in a vertical position. In this way, tipping is prevented and a stable position of the prototype is ensured, suitable for acquiring reliable measurements.

2.13 Costs

The total cost of the developed prototype was 1,139,056 COP, as summarized in Table 7. However, this value includes expenses specific to the experimental stage, such as design iterations, the use of commercial modules, and material waste.

Based on an optimization estimate of the system, it is projected that the production cost of the sensor can be reduced through a more efficient selection of components and design improvements, considering the experience gained during development. The optimized cost estimate is presented in Table 8, showing a significant reduction compared to the experimental prototype.

It is further estimated that the system cost can be reduced in a mass production scenario through optimization of the electronic and mechanical design. The adoption of components based on SMD technology would allow reducing the size of the PCB and the prototype in general, decreasing material usage and manufacturing costs. Although an exact quantification of this reduction is not available, these improvements are expected to have a significant impact on the economic feasibility of the system.

Table 7

Experimental prototype budget and material costs

Item	Unit	Price (COP)	Item	Unit	Price (COP)
AS7265X	1	227,656	BMP280	1	12,000
ESP32	1	22,000	DS18B20	1	15,000
LEDs 940 nm 1W	5	10,000	PCB	1	65,000
LEDs 495 nm 1W	5	11,200	Powerbank	1	60,000
LEDs 460 nm 1W	10	8,900	IRFZ44N	4	14,400
LEDs 590 nm 1W	10	14,300	Resistor 6.8 Ω	2	800
LEDs Full Spectrum	10	19,400	Resistor 4.7 kΩ	3	500
Silicone gaskets	8	43,000	Capacitor 100 nF	4	3,000
Acrylic sheets	5	8,200	Capacitor 1 μF	1	500
M5 screws	20	20,200	Capacitor 10 μF	2	1,000
M4 screws	10	11,500	M3 spacers	10	13,300
M5 nuts	22	14,500	M4 wing nuts	10	9,200
PG7 cable glands	10	11,000	3D printing	1	300,000
Laser cutting	1	27,000	Epoxy resin	1	85,000
Acetic silicone	1	22,000			
			TOTAL GENERAL (COP)		**1,139,056**

Note. All values are expressed in Colombian Pesos (COP) reflecting nominal local market distribution prices.

Table 8

Optimized prototype budget and component costs

Item	Unit	Price (COP)	Item	Unit	Price (COP)
AS7343	1	80,000	Powerbank 10,000 mA	1	60,000
ESP32	1	22,000	IRFZ44N	2	6,200
PETG	1	55,000	Resistor 6.8 Ω	2	800
LED Full Spectrum	1	2,000	Capacitor 100 nF	4	3,000
BMP280	1	12,000	Capacitor 1 μF	1	500
DS18B20	1	10,000	Capacitor 10 μF	2	1,000
PCB	1	65,000	Resistor 4.7 kΩ	3	500
Silicone gaskets	5	20,000	Resistor 10 kΩ	2	200
Acrylic sheets	2	3,300	Resistor 220 Ω	2	200
M5 screws	20	14,000	M3 screw and nut	4	2,200
M5 insert nuts	22	9,300	PG7 cable gland	1	1,000
Epoxy resin 500g	1	45,000			
			TOTAL (COP)		**413,200**

Note. Budget allocation for the optimized hardware iteration, leveraging a multi-channel spectral sensor to reduce total structural and component expenses.

2.14 Discussion

The obtained results support the feasibility of a multispectral absorption spectroscopy-based approach for dissolved oxygen estimation. The multiple linear regression model with Ridge regularization achieved an R^2 of 0.95 using median smoothing (15-sample window) and the 18 spectral bands, suggesting that the variables captured by the AS7265x sensor contain sufficient information to explain a large portion of the variability associated with DO concentration. This behavior is consistent with the findings reported by (Tran et al., 2024a), who proposed absorption spectroscopy as a viable alternative to fluorescence-based techniques, which often require more complex and expensive optical configurations. In this context, the obtained results demonstrate the potential of the proposed approach as a monitoring tool for aquaculture applications.

The sensitivity observed in the measurements to small variations in optical signal in-

tensity and acquisition highlights the importance of maintaining stable geometric conditions within the measurement system. Since the spectral response depends directly on the interaction between the light source, the medium, and the sensor, even minimal displacements between the emitting LED and the multispectral sensor can alter the distribution of received light and generate variations in the acquired signal. This behavior suggests that mechanical stability and optical alignment are key factors affecting the repeatability and robustness of the system.

Additionally, the current dimensions and geometry of the prototype may also influence its behavior during immersion. The need to incorporate additional weight to maintain device stability reveals limitations associated with the implemented physical design. In this context, more compact configurations could improve not only mechanical and optical stability but also the integration of the system into real-world continuous monitoring scenarios. In particular, a cylindrical geometry similar to a buoy could help reduce the risk of tipping and maintain more consistent measurement conditions during operation.

Although the obtained relative error (6.84%) and mean absolute error (0.29 mg/L) are higher than the values typically reported for high-precision reference electrochemical sensors, these results can be considered acceptable for applications focused on continuous monitoring and trend analysis. This is particularly relevant when considering the low-cost nature of the proposed prototype and its potential for further optimization through design improvements, more integrated manufacturing processes, and enhancements to the dissolved oxygen estimation model.

The performance degradation observed during tests conducted under modified conditions indicates a significant dependence of the model on the physicochemical conditions present during training. Variables such as sodium bisulfite concentration, temperature, reaction time, and mixture homogeneity affected the reproducibility of the acquired spectral signatures. Furthermore, the bisulfite used to reduce dissolved oxygen levels may introduce changes in the optical properties of the solution, modifying absorbance at specific wavelengths and generating spectral relationships that are not exclusively dependent on DO concentration. This could explain part of the performance loss observed when experimental conditions differ from those used during calibration.

In this regard, the results suggest that the relationship among dissolved oxygen concentration, temperature, light intensity, and spectral response may exhibit non-linear behavior. Although these variables were evaluated using a linear model, its generalization capability decreased under scenarios with environmental variations. This behavior indicates that the interactions within the system may not be fully described by linear relationships, particularly when simultaneous changes occur in the physicochemical and optical conditions of the measurement environment.

2.15 System impact

The developed system represents a low-cost alternative for dissolved oxygen estimation, which is relevant in applications such as aquaponics and water quality monitoring. Its implementation contributes to the development of accessible technological solutions in local contexts, facilitating the supervision of critical variables in productive systems. In particular, real-time estimation capability enables early detection of adverse conditions, which can reduce losses in aquaculture systems and optimize the use of aeration mechanisms.

From an economic and technological perspective, the prototype is positioned as a viable alternative to commercial sensors, promoting its adoption in small- and medium-scale systems. The integration of multispectral analysis techniques with real-time monitoring tools, together with the use of wireless connectivity, demonstrates the potential of electronic instrumentation and data processing in environmental applications. Likewise, continuous monitoring of dissolved oxygen allows more efficient management of water resources, contributing to the sustainability of aquaculture systems and to the mitigation of impacts associated with hypoxia conditions.

Conclusions

A multispectral-analysis-based optoelectronic system was designed, implemented, and validated for the estimation of dissolved oxygen in water, effectively integrating mechanical and electronic design with data processing tools. The prototype demonstrated the feasibility of using absorption spectroscopy as an alternative for measuring this variable in aquaculture applications.

The estimation model based on multiple linear regression made it possible to establish an effective relationship between spectral variables and dissolved oxygen concentration, achieving an average coefficient of determination of $R^2 = 0.9582$ and an error of $RMSE = 0.3801\,\text{mg/L}$. These results demonstrate an adequate fitting capability and good repeatability under the experimental conditions in which the model was trained and validated.

The system demonstrated stable behavior under conditions of high dissolved oxygen concentration, where the estimated values remained consistent with the reference values. In contrast, validation under low dissolved oxygen conditions presented limitations mainly attributable to the difficulty of recreating the physicochemical conditions of the training stage: variations in the concentration of the reducing agent, temperature, reaction time, and mixture homogeneity generate an environment that differs from the controlled calibration scenario.

From an economic perspective, the proposed system represents a low-cost alternative compared to commercial solutions, with high potential for further cost reduction through design optimization and mass production, favoring its accessibility for small and medium-scale producers.

Finally, the development demonstrates the potential of electronic instrumentation and IoT technologies for creating accessible solutions in water quality monitoring, contributing to the optimization of productive processes and the strengthening of sustainable aquaculture.

Recommendations

As a future improvement line, it is proposed to optimize the mechanical design of the system in order to improve watertightness and facilitate maintenance, especially in long-term operating environments. Likewise, it is suggested to implement more controlled methods for generating dissolved oxygen concentrations in laboratory conditions, allowing more precise and reproducible validation of the developed model.

Similarly, the possibility of reducing the number of wavelengths used is proposed, with the aim of simplifying the system without significantly compromising the model accuracy, through the use of variable selection techniques.

It is recommended to implement decoupling capacitors in the power supply lines to reduce noise and stabilize voltage. In particular, it is suggested to use 100 nF capacitors to filter high-frequency components, and capacitors between 1 µF and 10 µF to smooth low-frequency variations and transients, thereby contributing to improving the stability of system signals.

It is also proposed to implement non-linear models, such as MLP-type neural networks, optimized for real-time execution, in order to improve predictive capability and reduce error metrics such as RMSE or MSE. Likewise, it is suggested to expand the experimental database by incorporating measurements across different temperature ranges and to consider barometric pressure compensation, with the purpose of increasing the robustness and generalization capability of the model.

It is pertinent to explore alternative water deoxygenation methods that reduce dependence on the use of chemical agents, considering that the measured physical phenomenon is optical in nature. The use of sodium bisulfite may modify other physicochemical properties of the aqueous medium, in addition to dissolved oxygen, generating interference in the signals captured by the multispectral sensor and affecting the stability and reproducibility of the obtained measurements.

Bibliography

Agroguajira. (n.d.). Tilapia roja. https://www.agroguajira.com/index.php/especies/tilapia-roja

ams AG. (2018a). As7265x smart 18-channel vis to nir spectral id 3-sensor chipset datasheet.

ams AG. (2018b). *As7265x smart 18-channel vis to nir spectral sensor datasheet* [Accessed: 2026-04-15]. https://cdn.sparkfun.com/assets/learn_tutorials/8/3/0/AS7265x_Datasheet.pdf

Autoridad Nacional de Acuicultura y Pesca. (2013). *Diagnóstico del estado de la acuicultura en colombia*. Autoridad Nacional de Acuicultura y Pesca (AUNAP). Bogotá, Colombia. https://www.aunap.gov.co/documentos/OGCI/25-Diagn%C3%B3stico-del-estado-de-la-acuicultura-en-Colombia.pdf

Bosch Sensortec. (2018). Bmp280 digital pressure sensor datasheet.

Colprecios. (2026). *Trucha arco iris - precios en corabastos* [Consultado el 19 de abril de 2026]. https://colprecios.com/corabastos/carnicos/trucha-arco-iris

De Gerónimo, E., & Falomir Lockhart, L. J. (2022). Fluorescencia. In *Biofísica: Fundamentos y aplicaciones*. Universidad Nacional de La Plata. http://sedici.unlp.edu.ar/bitstream/handle/10915/153906/Documento_completo.pdf

Desun Uniwill. (2025). *What are the types of dissolved oxygen sensors used for measuring oxygen in water?* [Accessed: 2026-04-12]. https://disen-sensor.com/what-are-the-types-of-dissolved-oxygen-sensors-used-for-measuring-oxygen-in-water/

Espressif Systems. (2023). Esp32 series datasheet.

Food and Agriculture Organization of the United Nations. (2002). *Desarrollo y ordenación de la acuicultura: Situación actual, problemas y perspectivas*. FAO. https://openknowledge.fao.org/handle/20.500.14283/y3277s

Food and Agriculture Organization of the United Nations. (2024). *Versión resumida de el estado mundial de la pesca y la acuicultura 2024: La transformación azul en acción*. FAO. https://doi.org/10.4060/cd0690es

Food and Agriculture Organization of the United Nations. (n.d.). Mejora de la calidad de agua en los estanques. https://www.fao.org/fishery/static/FAO_Training/FAO_Training/General/x6709s/x6709s02.htm

GLOBE Program. (2005). Protocolo de oxígeno disuelto.

Gubbi, J., Buyya, R., Marusic, S., & Palaniswami, M. (2013). Internet of things (iot): A vision, architectural elements, and future directions [Including Special sections: Cyber-enabled Distributed Computing for Ubiquitous Cloud and Network Services Cloud Computing and Scientific Applications — Big Data, Scalable Analytics, and Beyond]. *Future Generation Computer Systems*, *29*(7), 1645–1660. https://doi.org/https://doi.org/10.1016/j.future.2013.01.010

Hamilton Company. (n.d.). *Optical dissolved oxygen sensors: Principles of operation*. Hamilton Company. Retrieved May 5, 2025, from https://www.hamiltoncompany.com/knowledge-base/article/optical-dissolved-oxygen-sensors-principles-of-operation

Hastie, T., Tibshirani, R., & Friedman, J. (2009). *The elements of statistical learning*. Springer.

Joint Committee for Guides in Metrology. (2008). Evaluation of measurement data — guide to the expression of uncertainty in measurement. https://www.bipm.org/en/publications/guides/gum.html

Junta Regional del Control de Calidad de Agua. (n.d.). Folleto informativo: Oxígeno disuelto (od) [Folleto informativo].

Laowisit, K. (2021). *Fresh shrimp on a white background* [Vecteezy. Consultado el 19 de abril de 2026]. https://es.vecteezy.com/foto/2129521-camarones-frescos-sobre-un-fondo-blanco

Li, F., Wei, Y., Chen, Y., Li, D., & Zhang, X. (2015). An intelligent optical dissolved oxygen measurement method based on a fluorescent quenching mechanism. *Sensors*, *15*, 30913–30926. https://doi.org/https://doi.org/10.3390/s151229837

Maxim Integrated. (2019). Ds18b20 programmable resolution 1-wire digital thermometer datasheet.

Medina, J. D., Castillo, E., & Rodríguez, L. (2022). Open-source low-cost buoy design for remote water quality monitoring in aquaculture. *PLoS ONE*, *17*(6), 1–21. https://doi.org/https://doi.org/10.1371/journal.pone.0269765

Miura, T., Tominari, Y., & Kondo, H. (2021). Dissolved oxygen measurement using optical absorption spectroscopy in the ultraviolet region. *Photonics*, *10*(5), 1–12. https://doi.org/https://doi.org/10.3390/photonics10050336

Montgomery, D. C., Peck, E. A., & Vining, G. G. (2012). *Introduction to linear regression analysis*. Wiley.

PriceSmart. (2025). *Tilapia roja fresca bandeja* [Consultado el 19 de abril de 2026]. https://www.pricesmart.com/es-pa/producto/tilapia-roja-fresca-bandeja-362893/362893

Recalde Mórtola, L. S. (2022). *Análisis comparativo de sensor óptico de oxígeno disuelto respecto al método de winkler para establecer la confiabilidad del instrumento* [Master's thesis, Escuela Superior Politécnica del Litoral].

SI Analytics GmbH. (2014). *Fdo 1100 ids: Sensor óptico de oxígeno – instrucciones de operación* [Código del documento: ba77044s01 03/2014]. SI Analytics GmbH. Mainz, Germany.

Silva, S., Costa, S. P. G., Pereira, M. M., & Coelho, P. J. (2016). Chlorophyll-based optical oxygen sensor obtained from natural sources for dissolved oxygen monitoring. *Sensors and Actuators B: Chemical*, *222*, 1150–1156. https://doi.org/https://doi.org/10.1016/j.snb.2015.09.080

Skretting. (s.f.-a). *Water quality management in black tiger shrimp aquaculture* [Recuperado el 28 de marzo de 2026]. https://www.skretting.com/en-in/blogs/water-quality-management-black-tiger-shrimp-aquaculture/

Skretting. (s.f.-b). *Water quality management in shrimp farming* [Recuperado el 28 de marzo de 2026]. https://www.skretting.com/en-in/blogs/water-quality-management-shrimp-farming/

Suárez, W. F. B., Castillo, E. R. R., & colaboradores. (2024). Sistema automatizado soportado en iot para monitoreo de calidad de agua en sistemas acuapónicos. *Ciencia y Desarrollo*, *15*(2), 45–58.

Super Global Calculator. (2024). Dissolved oxygen saturation formula. https://superglobalcalculator.com/formulas/environmental/dissolved-oxygen-saturation/

Taylor, J. R. (1997). *An introduction to error analysis*. University Science Books.

Tran, N. T., Pham, N. A. D., Nguyen, N. L., Nguyen, Q. B., Ha, C. T., & Nguyen, C. N. (2024a). Continuous monitoring of dissolved oxygen concentration using low-cost multispectral ...

Tran, N. T., Pham, N. A. D., Nguyen, N. L., Nguyen, Q. B., Ha, C. T., & Nguyen, C. N. (2024b). Continuous monitoring of dissolved oxygen concentration using low-cost multispectral sensors. *Journal of Science and Technique*, *2*(2), 64–76. https://doi.org/10.56651/lqdtu.jst.v2.n02.857.pce

U.S. Geological Survey. (2018). Dissolved oxygen and water. https://www.usgs.gov/water-science-school/science/dissolved-oxygen-and-water

Wei, Q., Li, B., Zhao, W., & Wang, Y. (2019). A critical review of dissolved oxygen measurement techniques. *Sensors*, *19*(18), 3995. https://doi.org/10.3390/s19183995

Zhang, Y., Yang, H., Gao, W., & Wu, C. (2024). Research progress of optical dissolved oxygen sensors: A review. *IEEE Sensors Journal*, *24*(19), 29564.

Appendices

In order to ensure the reproducibility of the developed system, the appendices corresponding to the different components of the project are included, such as the source code, implemented hardware, experimental data, and obtained results.

Due to the volume of information, these appendices are organized in a digital repository, which can be accessed through the following link:

https://drive.google.com/drive/folders/1az6Sxugoo1awW0O8awE8NR3JhMLLscEC

The structure of the appendices is as follows:

Appendix A. Code

Complete implementation in Arduino, Node-RED, Python, and integration with InfluxDB.

Appendix B. Hardware

Schematic and circuit design.

Appendix C. Experimental data

Raw datasets, filtered datasets, and data used for model training.

Appendix D. Video

Real-time demonstration of the system operation.

Appendix E. System

Configuration of the flow in Node-RED, integration with InfluxDB, and visualization in Grafana.

Appendix F. 3D modeling prototype

This section provides the STL files corresponding to the sealing elements and structural mechanical parts of the prototype.

Note on support tools: During the preparation of this document, artificial intelligence tools were used, specifically ChatGPT (OpenAI), as support for grammatical correction, improvement of writing, and technical translation of the text. The methodological development, acquisition of experimental data, and analysis of results correspond exclusively to the authors.